Probing Quantum Memory Effects in the Single Photon Regime

Carlos Belmonte[1], Frederik Vanden Berghe[1], Krassimir Panajotov[1,2], Thomas Durt[3*]

[1]B-Phot. Vrije Universiteit Brussel Pleinlaan 2, 1050 Brussel, Belgium.
[2]Institute of Solid State Physics, 72 Tzarigradsko Chaussee blvd., 1784 Sofia, Bulgaria.
[3]Aix Marseille Université, CNRS, Centrale Marseille, Institut Fresnel, UMR 7249, 13013 Marseille, France.
*Corresponding author: thomas.durt@centrale-marseille.fr

In this paper we study correlations present in experimental random series extracted from a Quantum Optical Random Number generator conceived and implemented in our lab. In particular we study the manifestations of inertia/memory effects. This study is realized in the single photon regime.

1 Introduction

We learn from classical and quantum physics that the future properties of a physical system are determined by its instantaneous, present state. This is reminiscent of the so-called Markov property in statistics, according to which* *"...the conditional probability distribution of future states of the process, given the present state and all past states, depends only upon the present state and not on any past states..."*

In previous papers (see [5] for a survey), one of us (T. D.) studied the possibility that quantum correlations exhibit non-Markovian features [4], in other words that quantum correlations would be endowed with an intrinsic, non-standard memory effect. Actually, several experiments were realized in the past, in different contexts, in order to test the possibility of such memory effects [2–4, 7]. These experiments aimed at testing hidden variable models (both local and non-local models [5]) which predicted the appearance of non-standard correlations between measurement outcomes collected at different times (different places in the case of non-local models [2]). We shall not enter in the detail of these experiments and models here, but instead we shall focus on the results of a statistical test that we developed in the past in order to characterize quantum random number generators that were developed at the Université Libre de Bruxelles (U.L.B.) and Vrije Universiteit Brussel (V.U.B.). We developed this test, from now on denoted the Histogram Inertia Indicator (H.I.I.) test in order to reveal whether histograms constituted from data measured at different times were correlated to each other.

Besides the aforementioned hidden variable models, we found inspiration in the idea of morphic resonance expressed and developed by Rupert Sheldrake [17] according to which the evolution of species and development of life in general are characterized by memory effects having as a consequence that new shapes/patterns tend to behave as attractors for other shapes/patterns. In a previous paper we showed that mixing Sheldrake's ideas and hidden variable models led to the prediction of observable non-standard memory effects (see [4] section 3: Sheldrake and Smolin's Models, and a Related Experimental Proposal).

*Quoted from Wiktionary.

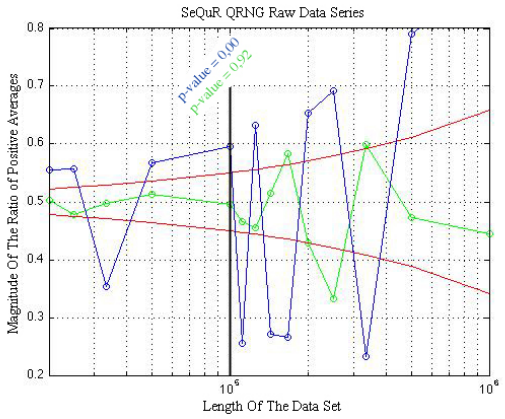

Fig. 1: SeQuR QRNG - Raw Data: A "near zone" effect is clearly present in the SeQuR data (blue graph). Successive histograms, each drawn from 1000 sequential random values, exhibit a manifest tendency to resemble each other. The green graph represents the same test on a Matlab pseudo-random series. The red lines represent the boundaries that are assigned to "perfect" random series. The plotted p-values confirm the results in graphical form. (quoted from [19])

Our main goal, when we developed the H.I.I. was to try and reveal whether quantum histograms would exhibit memory effects. It can be seen as an attempt to extrapolate the extent of validity of Sheldrake's ideas to the quantum realm.

A last source of inspiration was provided by the evidence for annual periodicity in decay data [9, 10] that has been revealed a few years ago. It has been suspected that this periodicity cannot be explained by environmental effects such as temperature, humidity, pressure, *etc* [11], nor is there a correlation with the Sun-Earth distance after re-analysation of the data [13].

All these observations suggest that there could exist some "regularity in randomness", some "hidden" pattern, a non-standard memory effect characterized by correlations between data collected at different times. This is a very upsetting and at the same time challenging idea which deserves to be considered seriously, from a foundational perspective [2–5, 7].

In particular we noticed the presence of an intriguing memory effect already some years ago [19], at the level of a random optical signal measured in the continuous counting

regime (see section 2.3). The data were delivered to us by colleagues from the U.L.B. developing a prototype of ultra-fast quantum optical random number generator [6]. Essentially, this device amplified fluctuations of the intensity delivered by a laser source. The results plotted at the level of Fig. 1 reveal for instance a clear deviation from the theoretical boundaries (in red) associated to a fully random process (without memory effect). We also checked in the same work [19] that Fourier filtering and/or Faraday filtering diminishes the effect, but does not suppress it totally. Our interpretation of these observations is that these correlations could be partially due to an external mechanism, and partially due to the internal memory of the device (here the light detector which is acting in the continuous (many photons) regime).

It was not clear however, uniquely on the basis of the observations, to decide whether the external source of the correlations had to be attributed solely to electromagnetic pollution (GSM devices, FM radio channels and so on) or whether it was necessary to resort to a universal memory effect in order to explain our observations.

Therefore we decided to test experimentally similar memory effects in the low intensity (single photon) regime, which was made possible by the development of quantum random number generators (QRNG) active in the low intensity (discrete counting) regime *in situ* in our labs and based on the random character of time delays between clicks collected with a single photon avalanche detector at the output of an attenuated laser source. The corresponding generator, the so-called Parity Quantum Optical Random Number (PQORN) generator has been described in a separate publication [6] and is briefly described in section 3.1 (see also Fig. 2).

As we shall describe in the present paper, we applied the H.I.I. test to the raw data generated with our PQORN generator. This program is triply challenging in our eyes because, as far as we know, nobody tested in the past the existence of memory effects by the same method, and *a fortiori* no such test has been achieved so far in the low intensity regime. Last but not least, if the memory effect revealed by the H.I.I. indicator is universal, its detection provides a criterion for discriminating physical randomness from pseudo-randomness which is a very challenging idea.

The paper is structured as follows. We describe in section 2 a new statistical test, the H.I.I. test, introduced in [19] aimed at measuring and/or revealing memory effects (section 2.1), as well as the corresponding p-value (section 2.2). Our methods are also relevant in the framework of random number generation because the H.I.I. test and the associated p-value are thus useful tools in order to characterize randomness.

Before scrutinizing (making use of the tests described in section 2) the existence of memory effects at the level of the PQORN generator (section 4), we investigated more in depth the correlations which appear in the high intensity regime at the level of our single photon detectors (section 3.2). These correlations are *a priori* not of quantum nature but they are induced by the dead time of the detector. As we show in section 4, in the high intensity regime, and only in this regime, the H.I. memory effect is present.

We also studied whether similar memory effects still exist beyond the near zone regime studied in section 4.1, and in particular whether non-local in space (section 4.2) and time (section 4.3) memory effects (previously denoted Spatial and Temporal Long Range Memory effects) can be measured at the level of our device. The last section is devoted to the conclusions and to the interpretation of the collected results.

2 The near-zone H.I.I. test

2.1 Qualitative test

In order to derive a statistical test aimed at revealing memory effects, we approached the problem as follows [19]: Each histogram of a given data sample – given it is not too large

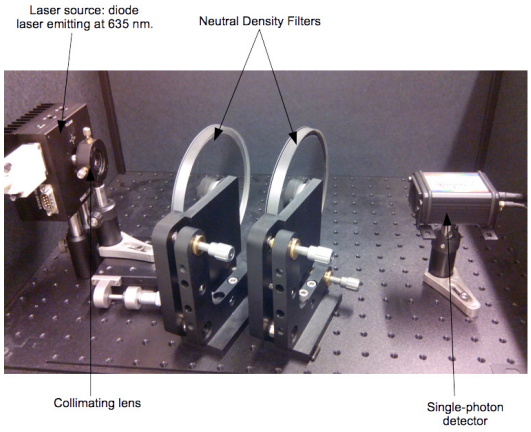

Fig. 2: Detailed setup for the near-zone experiment. It is composed of a laser source, two neutral density filters and a single photon detector. The same setup, supplemented with a nanosecond resolution clock constitutes the Parity QORNG.

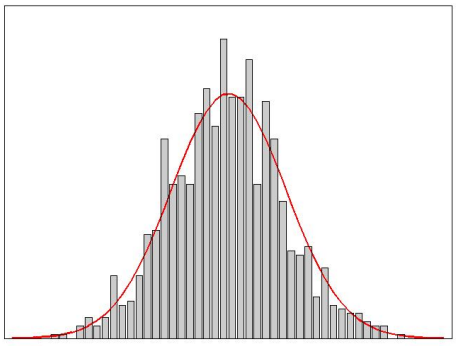

Fig. 3: Fluctuations of a sample histogram - constructed from 1 000 gaussian distributed random data values - around the line of the average histogram computed from a data sample of 10 000 000 gaussian distributed random values.

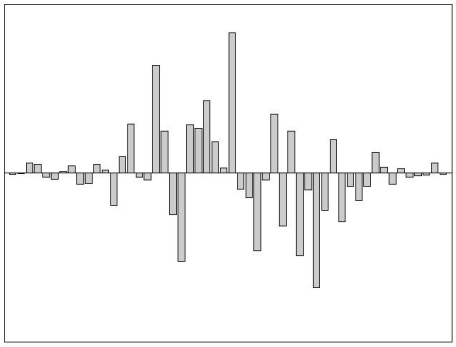

Fig. 4: The difference $\tilde{H}$ of a sample histogram H with the average histogram.

– fluctuates around the average histogram, which is obtained from a very large data sample, *cfr*. Fig. 3. For each histogram H we compute its difference with the mean histogram. This leaves us with a new normalized histogram $\tilde{H}$ in which each value can either have a positive of a negative value, depending whether that value is observed more or less often than in average, as shown in Fig. 4. Thereafter, we introduce a quantitative "resemblance" value r as follows. Consider $\tilde{H}_i$ and $\tilde{H}_j$ two neighboring histograms.

$$r_i = \sum_{\alpha} \tilde{H}_{i_\alpha} \tilde{H}_{j_\alpha} \quad \text{(with } j = i + 1\text{)} \tag{1}$$

with α the corresponding value of the histogram at this entry. Remark that we are working with histograms where values can be both positive and negative. Consequently, the inproduct r can be either positive or negative. The following interpretation can now be given to r:

- r **is large and negative**: Both histograms seem to be inverse of each other for most of the entries. The histograms have no near zone effect. Instead this suggests an anti- or complementary- "near-zone" effect.
- r **is close to zero**: Both histograms have approximately as much resemblance as difference. Again no "near zone" effect is observed.
- r **is large and positive**: Both histograms have the same shape for most of their entries. A "near zone" effect is then observed.

Considering that the random sequence of length n is divided in M data samples of length N, this analysis leaves us with $\lfloor \frac{N}{1000} \rfloor - 1$ values of r for each of the M samples, since we choose each histogram to be created from 1000 random values. Fig. 5 depicts graphical results after calculating all r-values.

This is only the first part of the investigation since, as one can deduce from Fig. 5, often, not much can visually be said about a possible "near-zone" effect. Therefore, it is appropriate to perform a statistical treatment of the data.

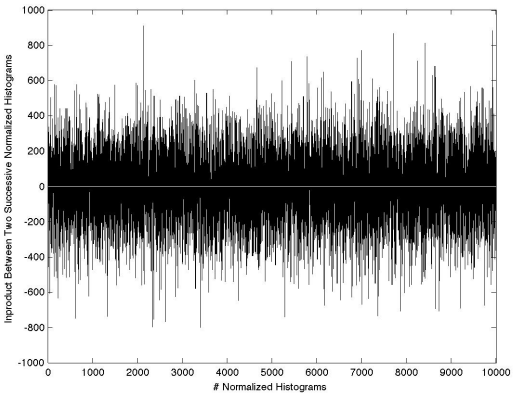

Fig. 5: Example graph of 9 999 inproducts between 10 000 successive histograms obtained from a data sample of $N = 10^7$ values.

Let us start by taking the average of all r inproducts:

$$\bar{r} = \frac{\sum_{i=1}^{\frac{N}{1000}-1} r_i}{\frac{N}{1000} - 1} . \tag{2}$$

Since the analysis is performed on M data samples of length N, each of the M samples now leaves us with one value of $\bar{r}$. These M average values $\bar{r}$ provide us with a qualitative indication of a "near zone" effect that we choose to express through the ratio of positive averages of $\bar{r}$, i.e.

$$\frac{\#\bar{r}_{pos}}{M} \tag{3}$$

with $\#\bar{r}_{pos}$ the amount of $\bar{r} \geq 0$. Note that the sign of $\bar{r}$ can be regarded as a Bernoulli process, or as a bit sequence with for example a bit value of 1 corresponding to a positive value and a bit value of 0 to a negative one. In a perfectly random process the ratio between them should be close to $1/2$ with a deviation depending on M, the amount of data samples. In order to determine the magnitude of this deviation we consider the law of large numbers to derive the boundaries:

$$\frac{\#\bar{r}_{pos}}{M} \sim \frac{1}{2} \pm \frac{\sigma_{bit}}{\sqrt{M}} = \frac{1}{2}\left(1 \pm \frac{1}{\sqrt{M}}\right) \tag{4}$$

with M the amount of data samples or the amount of values $\bar{r}$. For a data set of length n, $M = \lfloor \frac{n}{N} \rfloor$ so that the boundaries also depend on N.

It is expected for perfect random processes that the magnitude of the ratio of positive averages $\bar{r}$ will remain confined within the boundaries plotted in Fig. 6. One expects that sporadically $\bar{r}$ will be found outside the boundaries but in the case that it will remain persistently outside the boundaries we must suspect that the random sequence is biased. Considered so, we now have at our disposal a qualitative test aimed at testing the presence of the near zone effect. In the next section, we shall also derive a quantitative criterion, in the form of a p-value.

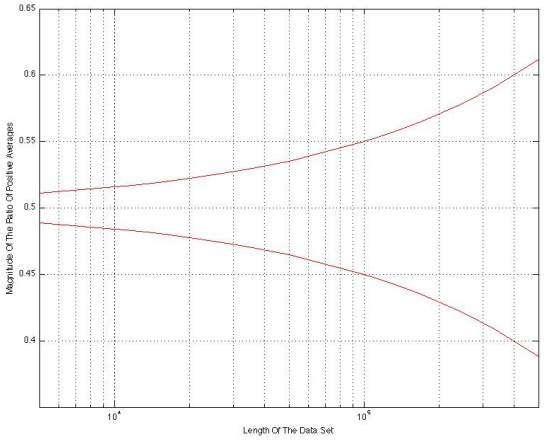

Fig. 6: Boundaries for the fluctuations of the ratio of positive averages $\bar{r}$ depending on M, the amount of data samples tested. Since a very large data sample is divided in M subsamples of length N, M decreases as N increases and consequently, the fluctuations also depend on the size N of the subsamples.

2.2 Derivation of a p-value for the near-zone H.I.I. test

The standard randomness tests (*e.g.* the NIST or Die Hard tests [12,16]) deliver their results through a so-called p-value. Typically, $p \in [0,1]$ is the probability of obtaining a test result at least as extreme as the one that was actually observed, assuming that the null hypothesis is true, *i.e.* the tested sequence is considered random. A p-value ≥ 0.01 indicates that the tested series of bits is random with a confidence interval of 99%. While the near-zone H.I.I. test described in the previous section is of qualitative nature and delivers its results in a graphical way, we shall now show how to connect a p-value to the different values in the graph of this near-zone H.I.I. test.

Recall that the value of $\bar{r}$ from (2) can be regarded as a Bernoulli process or conversely as a random walk if one considers a positive value of $\bar{r}$ as the value $+1$ and a negative value of $\bar{r}$ as -1. Consider the sequence $X = X_1, X_2, \ldots$ of values ± 1 in accordance to positive or negative values of $\bar{r}$. We define S_M as the sum

$$S_M = X_1 + X_2 + \ldots + X_M \tag{5}$$

with M the amount of values of $\bar{r}$ (see discussion at (2) and (3)). Compute the test statistics

$$Z = \frac{|S_M|}{\sqrt{2M}}\,. \tag{6}$$

Making use of the law of large numbers, the p-value can be shown [19] to be equal to

$$p\text{−value} = \operatorname{erfc}\left(\frac{Z}{\sqrt{2}}\right). \tag{7}$$

2.3 Near zone memory effect in the continuous counting regime

Some years ago [19], we investigated the existence of a memory effect at the level of an optical random number generator the SeQuR QRNG, acting in the continuous regime. Essentially, the device amplifies the fluctuations of the intensity delivered by a laser source [6]. We considered the decimal random data delivered by the detector. The tested results show clear similarities in the successive histograms from the data samples. This can be observed in Fig. 1, quoted from [19]. This analysis clearly indicates the presence of an inertia or memory effect in the signal. Let us now consider discrete data collected with single photon detectors.

3 Randomness in the low photon number regime

3.1 Parity QORNG

The *Parity QORNG* exploits the random nature of the distribution of clicks in a single photon detector. It is based on the parity of the time (in nanoseconds) for which the events (clicks) occur. If this time is even, the bit will be zero; if this time is odd, the bit will be one. The set-up to carry out this method consists of an attenuated laser source coupled to a single-photon detector (Fig. 2). The detector is coupled to a buffer via an acquisition card synchronized with a clock of high resolution (1 nanosecond).

As has been shown in [6], the principal advantages with this method are 1) that it requires to use only one photon-detector to generate a random number and 2) that even in the high intensity regime it delivers random series of very high quality*.

Before we characterize the H.I. effect, let us study the physical correlations exhibited by the single photon detectors of the parity QORNG.

3.2 Study of correlations due to dead-time of detectors

3.2.1 Successive clicks in one single-photon detector

In this section we will check the statistical properties of the data acquired in single-photon detectors in various regimes. These regimes are reached by modifying the attenuation of our two tunable attenuators (Fig. 2), from almost no attenuation at all to a high attenuation.

Before going further it is worth recalling that the single-photon detector is characterized by a dead time (that is to say the lapse of time during which the photon-detector will be off after detecting a photon) in the range of 45 to 50 ns. The resolution time of the acquisition card is 1 ns, therefore every 1 ns a datum will be acquired, while the maximum data that the acquisition card can memorize is 750 000 ns, after which the memory of the acquisition card is full.

*For instance bit series obtained from the PQORNG successfully pass [6] the NIST battery of standard randomness tests (frequency test, parity test, spectral test, entropy test and so on).

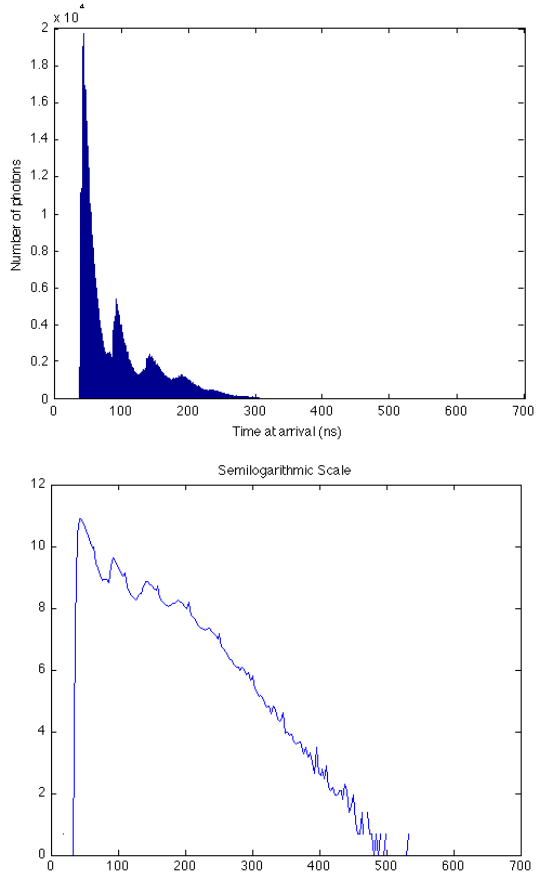

Fig. 7: Statistics of time arrival between photons in the high intensity regime. Average time between photons estimated to be more or less 36 ns.

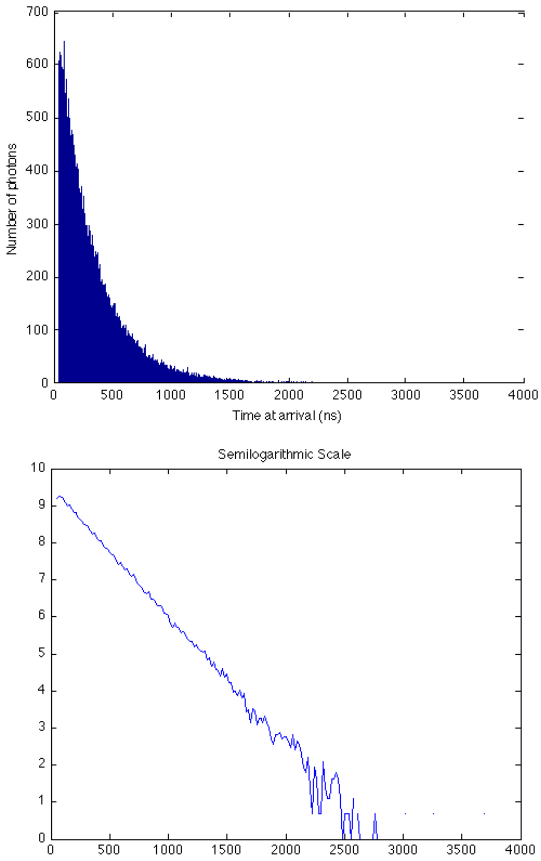

Fig. 8: Statistics of time arrival between photons in the low intensity regime. Average time between photons estimated to be more or less 294 ns.

Taking into account the specifications above, we performed a study of the time arrival between two photons in different regimes changing the attenuation. For instance, in the high intensity regime (low attenuation regime) we observe a distribution of delay times between clicks plotted in Fig. 7 which is contaminated by the correlations induced by the dead-time of the detector (as revealed by the presence of peaks separated by 45 ns). From the tail of the semi-logarithmic plot, we can infer the average time between two photons, which would be exactly the slope of the straight line if the distribution was Poissonian, which corresponds to a dead time equal to zero.

If in turn we work in a low intensity regime, for which the average time between two clicks is quite larger than the dead time of the detectors, we observe a nearly Poissonian distribution, as can be seen from Fig. 8. The single noticeable difference with a Poisson distribution is the null probability to measure successive clicks in a time smaller than the dead time (here 45 ns).

3.2.2 Simultaneous clicks in two single-photon detectors

In order to check the departure from the Poisson distribution, we estimated another parameter which is the number of simultaneous counts in two detectors placed at the output of a beamsplitter. When two photons arrive at the exact same time to the beamsplitter, there exist four possible scenarios (Fig. 9):

1. Both photons are detected by the photon-detector A.
2. Both photons are detected by the photon-detector B.
3. Photon A is detected by the photon-detector A and photon B is detected by the photon-detector B.
4. Photon A is detected by the photon-detector B and photon B is detected by the photon-detector A.

The probability of obtaining a single photon during a unit-period of time is (in case of a perfectly Poissonian distribu-

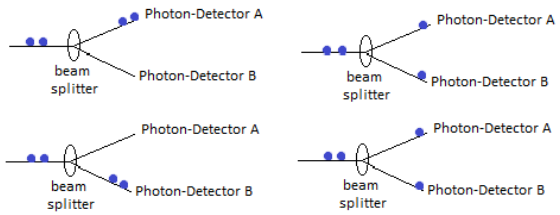

Fig. 9: Possibilities that two photons are detected by two photon-detectors.

tion):

$$P(\text{single}) = \frac{1}{\text{average time between photons}} \tag{8}$$

The probability of obtaining two photons at the input of the beamsplitter is then:

$$P(\text{pair}) = \left(\frac{1}{\text{average time between photons}}\right)^2 \frac{1}{2!} \tag{9}$$

Henceforth, the probability that two photons arrive during a same temporal window unity in the two photon-detectors can be calculated theoretically:

$$P(\text{double count}) = \left(\frac{1}{(\text{average time between photons})^2 \cdot 2!}\right)\frac{1}{2}$$

The average number of double clicks obeys therefore

$$N(\text{double counts}) = \left(\frac{\text{total number of photons}}{\text{average time between photons} \cdot 2!}\right)\frac{1}{2}$$

In the high intensity regime we found a significant departure from the Poisson distribution:

- Total number of photons $\approx 640\,000$.
- Average time between photons ≈ 21 ns.
- Simultaneous clicks in the 2 photon-detectors = 4 999.

$$\left(\frac{640\,000}{21 \cdot 2!}\right)\frac{1}{2} \approx 7\,619 \tag{10}$$

In the low intensity regime we found a better agreement:

- Total number of photons $\approx 184\,000$.
- Average time between photons ≈ 141 ns.
- Simultaneous clicks in the two photon-detectors = 272.

$$\left(\frac{184\,000}{141 \cdot 2!}\right)\frac{1}{2} \approx 326 \tag{11}$$

This confirms that when the dead time is small compared to the average time between two photons, the statistics of counts is Poissonian in good approximation, which fits with the standard quantum prediction for a coherently attenuated laser source. From this point of view, the limit of low intensities corresponds to the genuinely quantum regime, while in the high intensity regime (for which the dead time is comparable to the average time between two photons) quantumness is spoiled by correlations induced by the dead time mechanism of the detector.

Incidentally, our study also confirms that we nearly always operate in the single photon regime; the probability to have two photons or more in the same interval of acquisition (one nanosecond) being at most of the order of 10^{-2}, even in the "high" intensity regime.

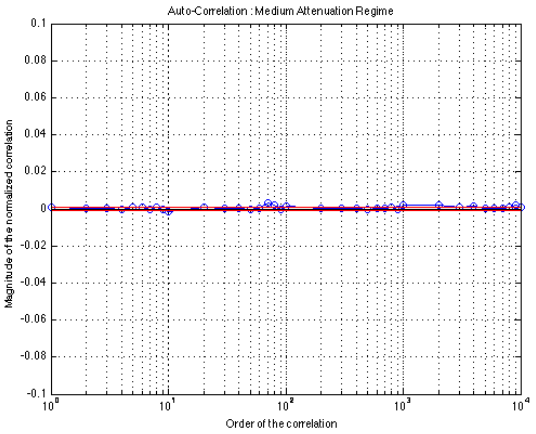

Fig. 10: Autocorrelation for the low intensity regime.

4 Characterization of the PQORN generator using the H.I.I. test

4.1 Near-zone temporal memory effect

The existence of a near-zone temporal memory effect would be revealed through the fact that similar histograms are significantly more probable to appear in the nearby (neighbouring) intervals of the time series of the results of measurements.

Using the setup in Fig. 2, we measured this effect in the two different regimes, the low intensity regime and the high intensity regime (they were defined in terms of the dead time at the end of the previous section).

To determine whether the effect is present, we make use of the H.I.I. test described in section 2, which delivers a p-value and a graph for a fast visual appreciation. We applied a level of significance of 0.01 for the p-value, hence if the p-value delivered is lower than the level of significance, we assumed that the presence of a significant memory effect gets confirmed by experimental data. Similarly, if the curve provided by the test remains outside the boundary curves, we assume that the existence of a memory effect is experimentally confirmed. We also used a standard auto-correlation test [6, 12, 16] to corroborate the results of the H.I.I. test.

4.1.1 Low intensity regime

We firstly measured the effect in the (highly attenuated) low intensity regime. We observed no correlation in this regime, as it is shown in Fig. 10. The H.I.I. test gives us the option to choose arbitrarily the sample length, which optimally ought to be of the order of the memory time of the H.I. effect. We selected four different sample lengths of 100, 300, 500 and 1000; and for each choice of a sample length, we tested the possible existence of a memory effect with the first, the second, the fifth and the tenth neighbour. For instance selecting 100 as a sample length, the reference sample runs from 1 to 100, the first neighbour sample from 101 to 200, the second neighbour one runs from 201 to 300, the fifth neighbour sam-

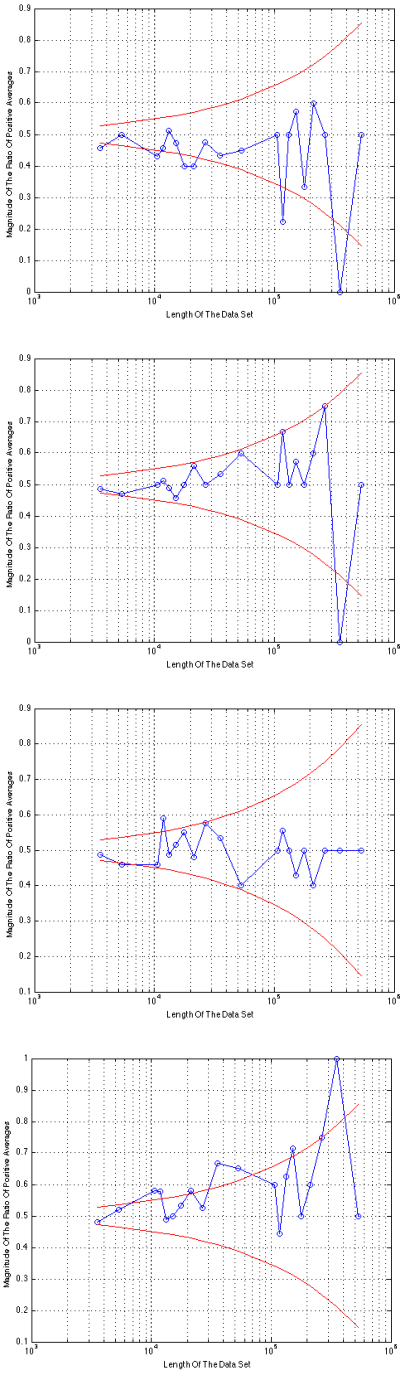

Fig. 11: Memory effect for the low attenuation regime with sample length of 100 for the first(a), the second (b), the fifth(c) and the tenth neighbour (d).

ple runs from 501 to 600 and so on. As is clear from Fig. 11, no memory effect is present in the low intensity regime. The result is also confirmed by similar plots obtained for sample lengths of 300, 500 and 1000 that we do not reproduce here in order not to overload the presentation. The corresponding p-values are gathered in Tab. 5. All the p-values are larger than

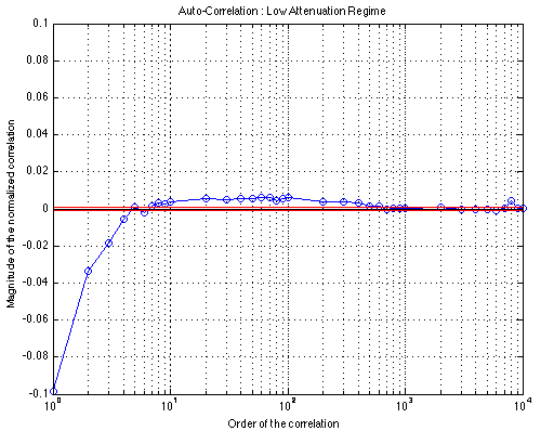

Fig. 12: Autocorrelation for the high intensity regime.

0.01, thus we can safely conclude that there is no memory effect in the low intensity regime, confirming the information provided by the graphics. These p-values are obtained by averaging all p-values associated to one "graphical" test.

4.1.2 High intensity regime

We measured again the correlations in the high intensity (weakly attenuated) regime and Fig. 12 shows that in this regime a strong auto-correlation prevails until the bit 600 approximately. We also measured the memory effect in the same way as for the low intensity regime, *i.e.* for different sample lengths (100, 300, 500 and 1000) and different neighbours (1^{st}, 2^{nd}, 5^{th} and 10^{th}). From Figs. 13, 14, 15 and 16, it can be seen that for a sample length of 100, the H.I. effect is present. On the other hand, for a sample length of 1000, the experimental curve stays inside the red boundaries most of the time. Actually, when two samples separated by less than say 1000 bits are compared, the memory effect is present, otherwise there is no H.I. effect. These results are corroborated by the auto-correlation (Fig. 12) which is strong until the bit 600 approximately. They also fit with the average p-values shown in Tab. 6.

4.2 Long range spatial H.I.-like correlations

In a previous paper [4], one of us (T. D.) predicted that similar histograms are highly probable to appear at different geographical points at the same time on the basis of a genuine quantum hidden variable model incorporating the morphic resonance concept of Sheldrake [17]. We conceived a new experiment in order to study this prediction, based on the setup of Fig. 17, which is composed of two sub-setups (sub-setup A and sub-setup B). Each sub-setup consists of one source, one neutral density filter and one photodetector and is equivalent to the set-up described in the previous section that we used for testing the near-zone effect. The two sources are launched at the same time. In a first time we implemented the same H.I.I.

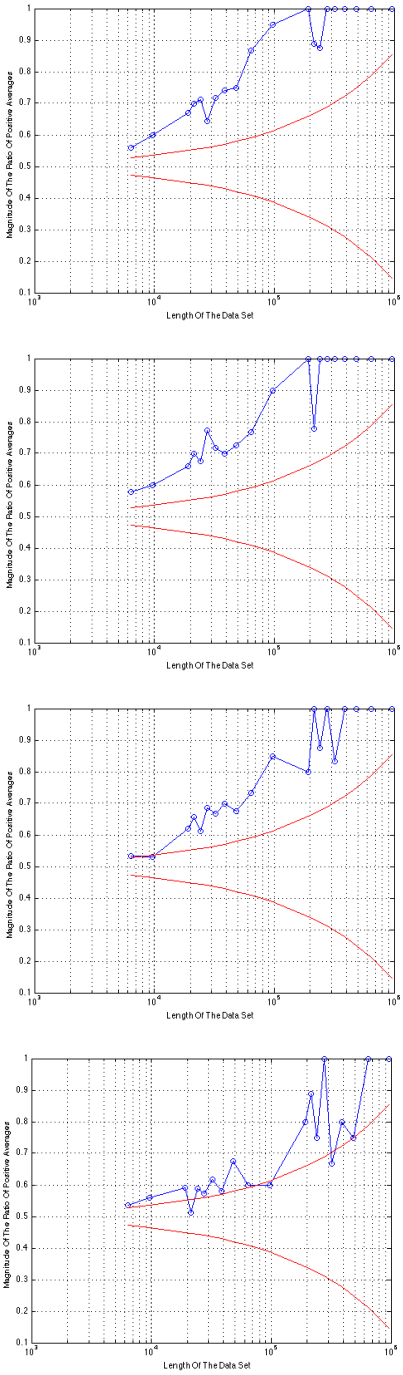

Fig. 13: Memory effect for the high intensity regime with sample length of 100 for the first (a), the second (b), the fifth (c) and the tenth neighbour (d).

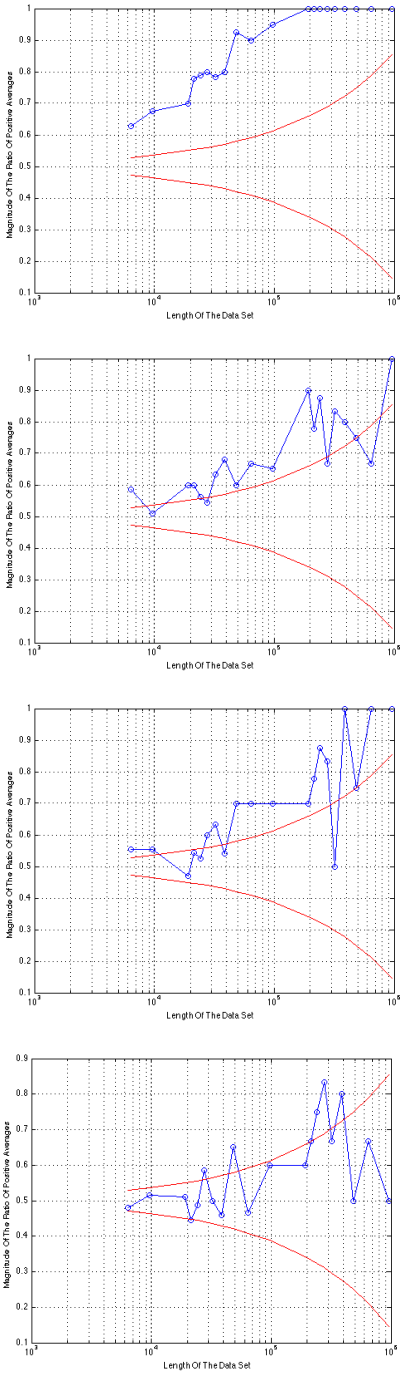

Fig. 14: Memory effect for the high intensity regime with sample length of 300 for the first (a), the second (b), the fifth (c) and the tenth neighbour (d).

test as in section 4.1 separately for each detector in order to check that each individual subset-up exhibits the near-zone memory effect. This can be seen for instance at the level of Tab. 1. The period of the near-zone memory effect is of the order of 500 clicks, as is corroborated by the auto-correlation tests in Figs. 18a and 18b.

In a second time, we adapted the H.I.I. test in order to be able to detect H.I.-like correlations between the two subset-ups. We have thus to compare the random series of time delays obtained in one photodetector (series A) with the random series obtained in the other photodetector (series B). Comparing both of them will determine whether the histograms are

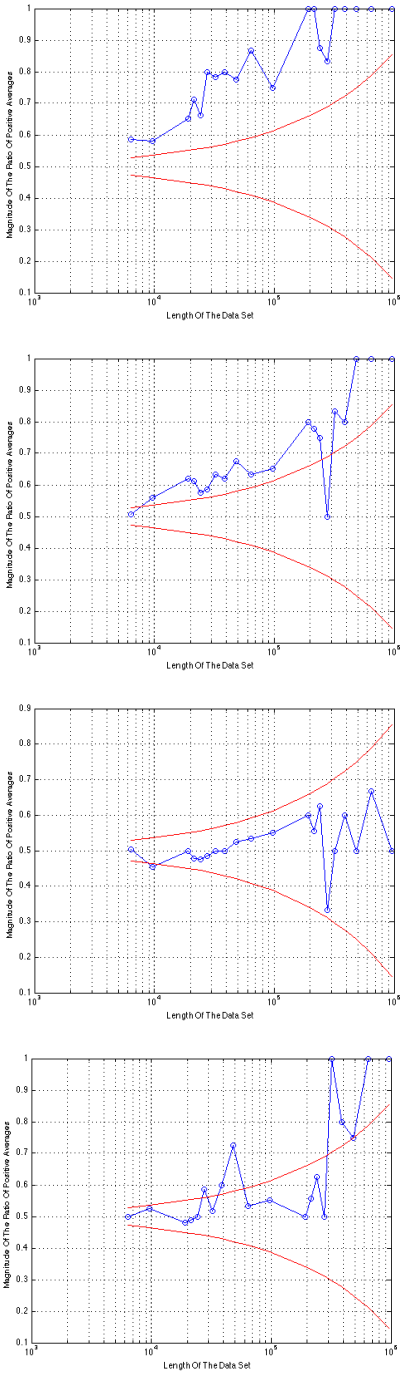

Fig. 15: Memory effect for the high intensity regime with sample length of 500 for the first (a), the second (b), the fifth (c) and the tenth neighbour (d).

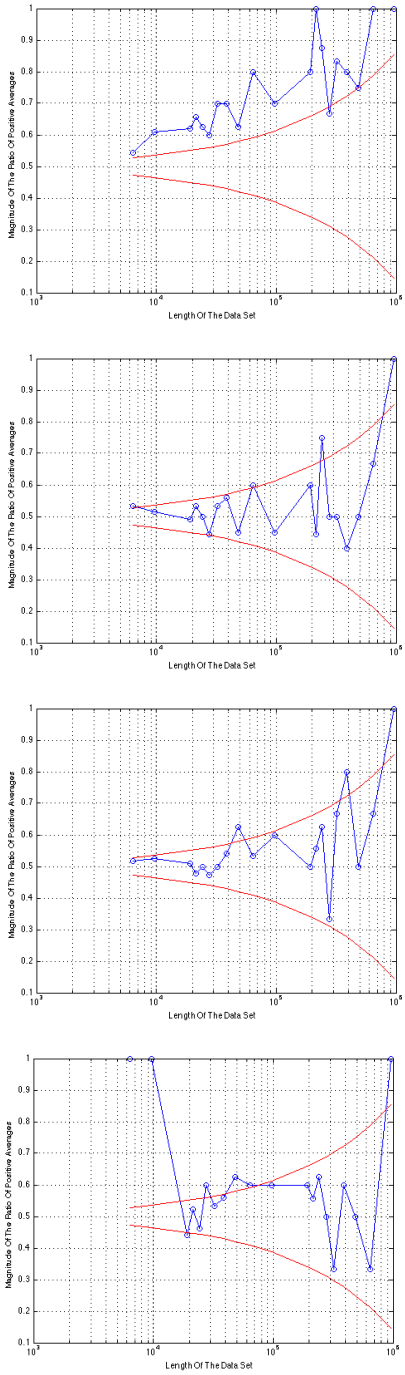

Fig. 16: Memory effect for the high intensity regime with sample length of 1000 for the first (a), the second (b), the fifth (c) and the tenth neighbour (d).

similar or not. In order to do so, a fixed sample length is selected (in our case, 100, 300, 500 and 1000) and we compare the histogram built from samples of this length extracted from series A with the corresponding histograms from series B, *i.e.* sample 1-100 of series A with the sample 1-100 of series B. We also compared neighbour histograms, like we did in section 4. This time we compare one histogram of series A with the neighbours of series B, *i.e.* for the first neighbour, sample 1-100 of series A with sample 101-200 of series B. We extended this procedure for the second, third, fifth, tenth and twentieth neighbour too. The results are encapsulated in Tab. 7. The average p-values are always quite larger than

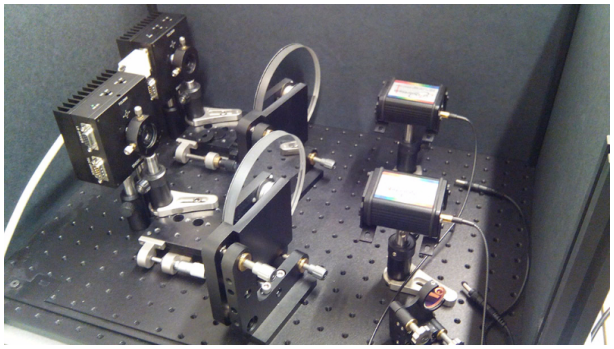

Fig. 17: Double set-up for detecting long range spatial H.I.-like correlations.

0.01, for all the cases, which shows that no observable spatial H.I.-like effect is present at the level of our experimental setup, even in the high intensity regime where individual setups exhibit a near zone memory effect. We checked by similar methods that in the low intensity regime no spatial H.I.-like effect is present. In both regimes we also scrutinized the graphical presentations of the test results (that we do not reproduce here in order not to overload the presentation), which confirmed the conclusions already drawn from the estimate of the p-values.

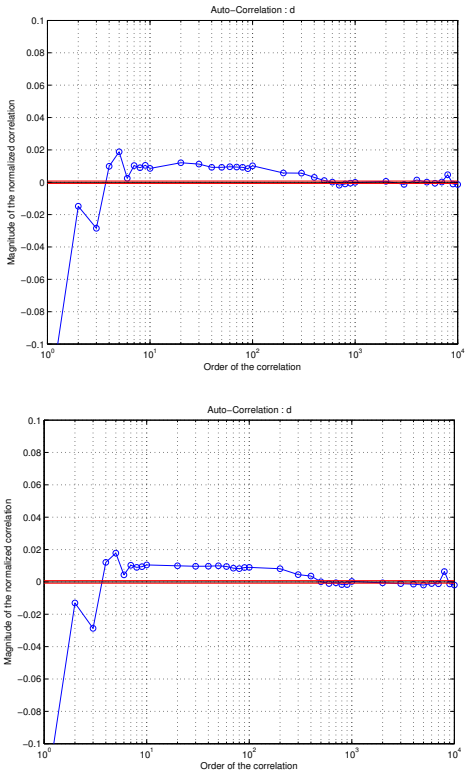

Fig. 18: Correlation for the data obtained in the two different photondetectors. Fig. (a) and Fig. (b) present a strong correlation.

Sample Length: 100	A	B
1 neighbor	0.0036	0.0033
2 neighbor	0.0071	0.0036
3 neighbor	0.0367	0.0094
5 neighbor	0.4984	0.3224
10 neighbor	0.4746	0.3269
20 neighbor	0.3191	0.3168

Tab. 1: p-values for the two sub-setups with a sample length of 100 bits for different neighbours (first, second, third, fifth, tenth and twentieth.

4.3 Long range temporal memory effects

The aforementioned periodic modulation of radio-active emission with a period of about 365 days [9, 10], suggests that the phenomenon has a cosmophysical origin. We therefore investigated the possibility to generalize these observations in the case of a quantum signal. We focused on the 24-hour period experiment due to the large amount of time that we would have spent in tracking yearly memory effects. The 24-hour period would be an indication of the existence of an external agent that influences the object of study, most probably the rotation of the Earth. Our aim was to probe the existence of this effect at the level of the quantum signal obtained from our QRNG. For our experiment we used the same setup as in the near-zone experiment in section 4. It consists again of a laser source, a collimating lens, two neutral density filters and one avalanche photo-diode.

In February 2015, we realized a series of experiments, after having synchronized our computer clock with an atomic clock from the nist.gov website* in such a way that all the measurements were automatized. Then, the runs were performed at exactly the same time every day for three consecutive days and we performed 20 different experimental runs with an interval of 20 second between each of them†.

We estimated, based on the slope of the semi-logarithmic plot of the histogram of delay times, the average time delay and we found that the drift was small, with average times comprised in the interval 45-52 ns. Thereafter we estimated the individual H.I.I. p-values which measure the cross-correlations between the samples of days 1 and 2, of days 2 and 3, and of days 1 and 3. The results are encapsulated in Tab. 2.

*The procedure for doing so is available on the website http://www.nist.gov/pml/div688/grp40/its.cfm

† We learn from wikipedia that... *"A synodic day is the period it takes for a planet to rotate once in relation to the body it is orbiting. For Earth, the synodic day is known as a solar day, and is about 24 hours long. The synodic day is distinguished from the sidereal day, which is one complete rotation in relation to distant stars. A synodic day may be "sunrise to sunrise" whereas a sidereal day can be from the rise of any star to the rise of the same star on the next day. These two quantities are not equal because of the body's movement around its parent"...* Henceforth we expect a difference between the sidereal and synodic (solar) day to be of the order of 24x3600/365 second, more or less 240 second. Our measurements cover 400 second, which allows us to address at the same time the synodic and sidereal periods

Total number of p-values: 3380
Day 1 Day 2
Number p-values < 0.01 = 272
Number p-values < 0.1 = 978
Day 2 Day 3
Number p-values < 0.01 = 284
Number p-values < 0.1 = 980
Day 1 Day 3
Number p-values < 0.01 = 221
Number p-values < 0.1 = 988

Tab. 2: Statistics of "pathological" p-values, from consecutive random series separated by 24 or 48 hours.

Total number of p-values: 8000
Day 1 Day 2
Number p-values < 0.01 = 123
Number p-values < 0.1 = 1195
Day 2 – Day 3
Number p-values < 0.01 = 152
Number p-values < 0.1 = 1201
Day 1 – Day 3
Number p-values < 0.01 = 104
Number p-values < 0.1 = 1185

Tab. 3: Statistics of "pathological" p-values, from pseudo-random series.

There were 13 runs each day and from each pair of runs we extracted twenty p-values (each of these values is associated to a point on a graph similar to, for instance, the plots in Fig. 11). By doing so, for each pair of days, we were able to estimate 13 times 13 times 20 = 3380 p-values from the cross-correlations between samples extracted at different days.

In order to properly calibrate the statistical distribution of p-values we did two things:

A) we generated sixty runs of Poisson distributed time series characterized by an average time of the order of 50 ns. The duration of each series was the same as the duration of each experimental run. We arbitrarily assigned a day to each of them, according to the rule 1-20 → day 1, 21-40 → day 2, 41-60 → day 3. Then we considered the 400 (20 times 20) cross-correlations between the data "extracted at different days" and estimated the corresponding p-values, following the same algorithm already used for establishing Tab. 2. The results are encapsulated in Tab. 3.

B) We also estimated through the same method the H.I. cross-correlation between samples that were measured in June 2014 and those measured in February 2015. Here again there were three runs of 13 samples, measured at different days, after a period of the order of 24 hours each time, and also in the high intensity regime, but the timing of the data collected in June 2014 was not automated. We estimated correlations between data measured in days 1, 2 and 3 in June 2014 and those measured in days 1, 2 and 3 in 2015. The results are summarized in Tab. 4.

Total number of p-values: 3380
Day 1 in June 2014 Day 1 in February 2015
Number p-values < 0.01 = 112
Number p-values < 0.1 = 578
Day 2 in June 2014 Day 1 in February 2015
Number p-values < 0.01 = 82
Number p-values < 0.1 = 526
Day 1 in June 2014 Day 3 in February 2015
Number p-values < 0.01 = 91
Number p-values < 0.1 = 521

Tab. 4: Statistics of "pathological" p-values, from consecutive random series measured in June 2014 and February 2015.

For obvious reasons, we consider that the statistical distribution of "pathological" p-values which appears in Tabs. 3 and 4 is representative of uncorrelated data. Indeed, pseudo-random series do not exhibit any memory effect, and we do not expect that data measured in June 2014 and February 2015 are correlated. This is confirmed by a comparison of those tables: if we consider the occurrence of p-values smaller than 0.1, we find a probability of the order of 0.15 in each case*.

On the contrary, in Tab. 2 the occurrence of p-values smaller than 0.1 is of the order of 0.29, twice more, which reveals the existence of a systematic memory effect, persisting after 24 hours. We consider therefore that our observations confirm the existence of long range temporal H.I.-like correlations of periodicity of the order of 24 hours, which appears, at least in our eyes, to be a very surprising result.

5 Conclusions and discussions

In this paper we studied the H.I. effect, which, roughly, would manifest itself through a tendency of random series to present analogous departures from their mean statistical behaviour. This tendency would possibly characterize data collected in the same temporal interval (what we denoted the near zone memory effect) but could present non-local features (non-local in time and/or space), what we denoted the long range temporal (resp. spatial) memory effect.

Our main goal was to study experimentally whether or not a memory effect of the H.I. type was present in the single photon regime. We developed a new, self-cooked algorithm, described in section 2 in order to realize this objective.

*At first sight we ought to expect 0.1 instead of 0.15, but we must have in mind that the p-value derived by us corresponds to a situation where the sign of the parameter r defined at the level of (1) was negative in exactly fifty percent of the cases and positive in fifty percent of the cases, which is of course an assumption that is not always strictly verified. From this point of view, the p-value defined by (7) ought not to be considered as an exact p-value but still plays the role of a valuable indicator.

Sample Length	1^{st} Neighbor	2^{nd} Neighbor	5^{th} Neighbor	10^{th} Neighbor
100	0.4762	0.6031	0.6048	0.3997
300	0.4515	0.5647	0.4537	0.5269
500	0.5323	0.3049	0.4101	0.4614
1000	0.4105	0.4745	0.5121	0.2665

Tab. 5: p-values extracted from the H.I. test for the low intensity regime for different sample lengths and different neighbours.

Sample Length	1^{st} Neighbor	2^{nd} Neighbor	5^{th} Neighbor	10^{th} Neighbor
100	0.0037	0.0043	0.0219	0.1005
300	0.0033	0.1100	0.1489	0.4066
500	0.0042	0.1098	0.6511	0.4410
1000	0.0304	0.4866	0.4876	0.3305

Tab. 6: Parity Method: Results of the file generated with the Split Method applying the NIST test battery.

Sample length	0^{th} neighbour	1^{st} neighbour	2^{nd} neighbour	3^{rd} neighbour	5^{th} neighbour	10^{th} neighbour
100	0.4330	0.5725	0.4067	0.4844	0.4530	0.5348
300	0.4608	0.5303	0.2870	0.2363	0.3765	0.3965
500	0.4508	0.4930	0.5378	0.4623	0.3572	0.0361
1000	0.5029	0.4965	0.4373	0.3953	0.2483	0.1399

Tab. 7: p-values when series A and B are compared for different sample length (100, 300, 500 and 1000 bits) for different neighbours (first, second, third, fifth, tenth and twentieth.

Our conclusions are the following:

A) The near-zone H.I. memory effect is well present in the single photon regime, but only in the high intensity regime (for which the dead time is comparable to the average time between two photons). As we discussed in section 3.2, the limit of low intensities (when the dead time is quite larger than the average time between two photons) corresponds to the genuinely quantum regime, and in this regime no memory effect is present. This goes in the sense of the conclusion [19] drawn from the study of the SeQuR QORNG, for which the H.I. effect could be explained in terms of external electromagnetic pollution, combined with an internal memory time (inertia) of the photodetector. The persistence of H.I.-like correlations after 24 hours (that we address below) is however more difficult to explain. Anyhow, we can safely conclude from our experiments and our analysis that "pure" quantum random series, collected in the low intensity single photon regime do not exhibit any kind of observable H.I.-like correlation.

B) We were unable to observe manifestations of a long range spatial memory effect but detected a systematic tendency indicating the possible presence of the long range temporal memory effect, even after 24 hours. Our preliminary result ought to be of course confirmed by supplementary studies. The door remains thus open for what concerns the "daily" effect. It is worth noting that, even if this effect gets definitively confirmed, its interpretation is not straightforward. It is well-known for instance that some noises in nature (and in particular at the surface of our planet) exhibit a 24 hours period. It could be that the daily memory effect merely reveals this feature.

In any case, we hope that, beside contributing to a better understanding of fundamental aspects of quantum randomness*, our study also brings new tools aimed at characterizing randomness in general. We actually consider that the H.I.I. test provides a new statistical test, complementary to the standard NIST tests, and in particular to the auto-correlation test.

As we have shown (*e.g.* in section 4.1.2), at the level of physical random number generators, when auto-correlation is present, the H.I. effect is most often present too, which is already remarkable in itself and suggests the existence of a universal memory effect.

Moreover, as shown in section 4.3, the long range temporal H.I. effect provide an example where the H.I.I. test reveals a systematic tendency, even in absence of auto-correlation (we checked for instance that the auto-correlation between data collected at different days (1,2,3) was uniformly flat).

We are still far away from one of our initial motivations, which was to be able to discriminate between physical randomness and pseudo-randomness thanks to the H.I.I. test†,

*In particular the main motivation of one of us (T. D.) was to investigate possible memory effects at the level of the quantum statistics, and finds its place in a series of works centered around this question [2–5, 7]

†In certain cases, pseudo-randomness can be revealed by measuring the

and the low intensity case provides a counterexample to the mere possibility of doing so in general, but at least, our measurements confirmed that the H.I. effect is present in nature in various regimes. In particular it is weakened but still present after a delay of 24 hours, which is very amazing. Therefore we are intimately convinced that it is important to pursue these investigations. For instance it would be interesting in the future to compare results obtained with our algorithm and those obtained by Shnoll and coworkers, making use of a quite different algorithm [8,14,18], and applying it to noise [15], not to quantum signal as we did, which addressed relatively short series of data (of the order of 30 clicks only), contrary to ours, where we systematically made use of the law of large numbers in order to estimate p-values.

Last but not least, it would be interesting to study the appearance of the H.I.-effect at various temporal and spatial scales, the present work constituting only a first probe in this direction.

Acknowledgements

Support from the B-Phot team, to his leader Hugo Thienpont, and the ICT Impulse Program of the Brussels Capital Region (Project Cryptasc) is acknowledged. Sincere thanks to Marco Bischof for drawing attention of one of us (T.D.) on Shnoll's work, some years ago.

Submitted on August 16, 2016 / Accepted on October 9, 2016

References

1. Calude C. S., Dinneen M. J., Dumitrescu M., and Svozil K. Experimental Evidence of Quantum Randomness Incomputability. *Physical Review A*, 2010, v. 82 (022102).
2. Durt T. About the Possibility of Supraluminal Transmission of Information in the Bohm-Bub Theory. *Helvetica Physica Acta*, 1999, v. 72, 356.
3. Durt T. Do Dice Remember? *International Journal of Theoretical Physics*, 1999, v. 38, 457.
4. Durt T. Quantum Mechanics and the Role of Time: Are Quantum Systems Markovian? *International Journal of Modern Physics B*, 2012, v. 26 (27&28), 1243005.
5. Durt T. Do Quantum Dice Remember? in Aerts D., Aerts S., and de Ronde C., eds. Probing the Meaning of Quantum Mechanics. World Scientific, Singapore, 2014, 1–24.
6. Durt T., Belmonte C., Lamoureux L-P., Panajotov K., Vanden Berghe F., and Thienpont H. Fast Quantum-Optical Random-Number Generators. *Physical Review A*, 2013, v. 87, 022339.
7. Durt T., Mathevet R., Robert J., and Viaris de Lesegno B. Memory Effects in Atomic Interferometry: A Negative Result, in Aerts D., Czachor M., Durt T., eds. Entanglement, Non-linearity, Quantum Structures and New Experiments, 2000, 165–204.
8. Fedorov M. V., Belousov L. V., Voeikov V. L., Zenchenko T. A., Zenchenko K. I., Pozharskii E. V., Konradov A. A., and Shnoll S. E. Synchronous Changes in Dark Current Fluctuations in Two Separate Photomultipliers in Relation to Earth Rotation. *Astrophysics and Space Science*, 2003, v. 283, 3–10.
9. Fischbach E., Buncher J. B., Gruenwald J. T., Jenkins J. H., Krause D. E., Mattes J. J., and Newport J. R. Time-Dependent Nuclear Decay Parameters: New Evidence for New Forces? *Space Science Review*, 2009, v. 145, 285–335.
10. Jenkins J. H., Fischbach E., Buncher J.B., Gruenwald J. T., Krause D. E., and Mattes J. J. Evidence of Correlations Between Nuclear Decay Rates and Earth-Sun Distance. *Astroparticle Physics*, 2009, v. 32, 42–46.
11. Jenkins J.H., Mundy D.W., and Fischbach E. Analysis of Environmental Influences in Nuclear Half-Life Measurements Exhibiting Time-Dependent Decay Rates. *Nuclear Instruments and Methods A*, 2010, v. 620 (2–3), 332–342.
12. Marsaglia G. The Marsaglia Random Number CDROM Including the Diehard Battery of Tests of Randomness, 1995, http://www.stat.fsu.edu/pub/diehard/.
13. Norman E. B., Browne E., Shugart H. A., Joshi T. H., and Firestone R. B. Evidence Against Correlations Between Nuclear Decay Rates and Earth-Sun Distance. *Astroparticles Physics*, 2009, v. 31, 135–137.
14. Panchelyuga V. A., Kolombet V. A., Panchelyuga M. S., and Shnoll S. E. Local-Time Effect on Small Space-Time Scale. arXiv: physics/0610137.
15. Rabounski D. and Borissova L. General Relativity Theory Explains the Shnoll Effect and Makes Possible Forecasting Earthquakes and Weather Cataclysms. *Letters to Progress in Physics*, 2014, v. 10 (2), 63–70.
16. Rukhin A., Soto J., Nechvatal J., Smid M., Barker E., Leigh S., Levenson M., Vangel M., Banks D., Heckert A., Dray J., and Vo S. Statistical Test Suite for Random and Pseudorandom Number Generators for Cryptographic Applications. NIST Special Publication, 2001, v. 800-22.
17. Sheldrake R. Une nouvelle science de la vie. Eds. du Rocher, Monaco, 1985.
18. Shnoll S. E., Colombet V. A., Pozharskii E. V., Zenchenko T. A., Zvereva I. M., and Konradov A. A. Realization of Discrete States During Fluctuations in Macroscopic Processes, *Physics-Uspekhi*, 1998, v. 43 (2), 1025–1035.
19. Vanden Berghe F. Quantum Aspects of Cryptography: From Qutrit Symmetric Informationally Complete Projective Operator Valued Measure Key Encryption to Randomness Quality Control. Ph.D. thesis, Vrije Universiteit, Brussels, 2011.

algorithmic complexity of a pseudo-random series, which delivers by then a criterion for discriminating quantum randomness from pseudo-randomness because, as has been shown elsewhere [1], quantum random series are incompressible.